PROCEEDINGS OF SCIENCE

Resistive Relativistic Simulations of Astrophysical Jets

Giancarlo Mattia,[a,*] **Luca Del Zanna,**[a,b] **Matteo Bugli**[c,d,e] **and Andrea Mignone**[c]

[a] *INFN, Sezione di Firenze,*
Via G. Sansone 1, I-50019 Sesto Fiorentino (FI), Italy
[b] *Dipartimento di Fisica e Astronomia, Università di Firenze,*
Via G. Sansone 1, I-50019 Sesto Fiorentino (FI), Italy
[c] *Dipartimento di Fisica, Università di Torino,*
Via P. Giuria 1, I-10125 Torino, Italy
[d] *Université Paris-Saclay, Université Paris Cité, CEA, CNRS, AIM,*
F-91191, Gif-sur-Yvette, France
[e] *INFN, Sezione di Torino,*
Via P. Giuria 1, I-10125 Torino, Italy

E-mail: mattia@fi.infn.it

We present a systematic numerical study of the propagation of astrophysical magnetized relativistic jets, in the context of resistive relativistic magnetohydrodynamics (RRMHD) simulations. Simulations are obtained with the PLUTO code. We investigated different values and models for the plasma resistivity coefficient, assessing their impact on the level of turbulence, the formation of current sheets and reconnection plasmoid, and the electromagnetic energy content.

High Energy Phenomena in Relativistic Outflows VIII (HEPROVIII)
23-26 October, 2023
Paris, France

*Speaker

PoS(HEPROVIII)073

1. Introduction

Astrophysical jets represent a ubiquitous phenomenon in the Universe, characterizing various classes of celestial sources at very different spatial scales and evolutionary stages. The electromagnetic spectral signature of such objects often features highly non-thermal radiation, mostly synchrotron and inverse Compton processes, due to accelerated relativistic particles (electrons). Different processes have been invoked to explain such particle acceleration in astrophysical sources. In particular, relativistic magnetic (fast) reconnection, i.e. the impulsive topological rearrangement of field lines in a magnetically dominated or very hot plasma [1, 2] has been extensively investigated in recent years. Due to the unavoidable numerical resistivity present in every numerical simulation, the disentanglement of the effects due to the truncation error from the physical process is a key point to understand the role of magnetic reconnection in astrophysical jets. In the present work (which is mostly taken from Mattia et al. 5) we perform and discuss high-resolution axisymmetric simulations of jets propagating in a uniform magnetized medium. Simulations are obtained with the PLUTO shock-capturing code [6]. Regions of high values of the current density and the possible sites for particle acceleration inside current sheets are singled out, zooming promising regions with evolving plasmoids in selected cases. We show that our combination of numerical algorithms can ensure robustness for the variety of the explored parameters and highly accurate results, in terms of small-scale turbulent features and reconnection sites.

2. Numerical setup

We solve the equations of Resistive Relativistic Magnetohydrodynamics (RRMHD) [7], which consist of mass, momentum, and energy conservation laws coupled with Maxwell equations. The closure is provided by employing the Taub equation of state [8]. The RRMHD equations consist of a set of hyperbolic partial differential equations (reported, e.g., in Del Zanna et al. 1, Mattia et al. 5) with a stiff source term in Ampere's law (for the evolution of the electric field)

$$\frac{\partial \vec{E}}{\partial t} - \nabla \times \vec{B} = -(\nabla \cdot \vec{E})\vec{v} - \eta^{-1}\gamma[\vec{E} + \vec{v} \times \vec{B} - (\vec{E} \cdot \vec{v})\vec{v}]$$

where η is the magnetic resistivity, $\vec{E}$ and $\vec{B}$ are, respectively, the electric and magnetic field and $\vec{v}$ is the fluid velocity (with Lorentz factor γ). The resistivities here adopted yield an evolutionary time scale for the electric field which is orders of magnitude shorter than the ones typical for the other variables, ruling out purely explicit Runge-Kutta schemes. Therefore we adopt a combination of parabolic reconstruction, HLL Riemann solver, and IMEX-SSP(332) Runge-Kutta scheme [9] to provide the best combination of accuracy and robustness.

Here we consider a 2D axisymmetric setup in cylindrical coordinates (r, ϕ, z) and uniform grid over a domain of $r \in [0, 25r_j]$ and $z \in [0, 50r_j]$ with a resolution of 1200×2400 computational zones. The magnetized relativistic jet is injected into the domain from the lower boundary ($z = 0$) in the region $r < r_j$, where $r_j = 1$ is the characteristic length used for normalization, corresponding to 48 grid cells in both r and z directions. The jet is initialized with uniform density $\rho_j = 1$ and vertical velocity specified by the Lorentz factor $\gamma_j = 10$. Its magnetic field structure is the same as in Mignone et al. [10], consisting of a variable toroidal component and a constant vertical component.

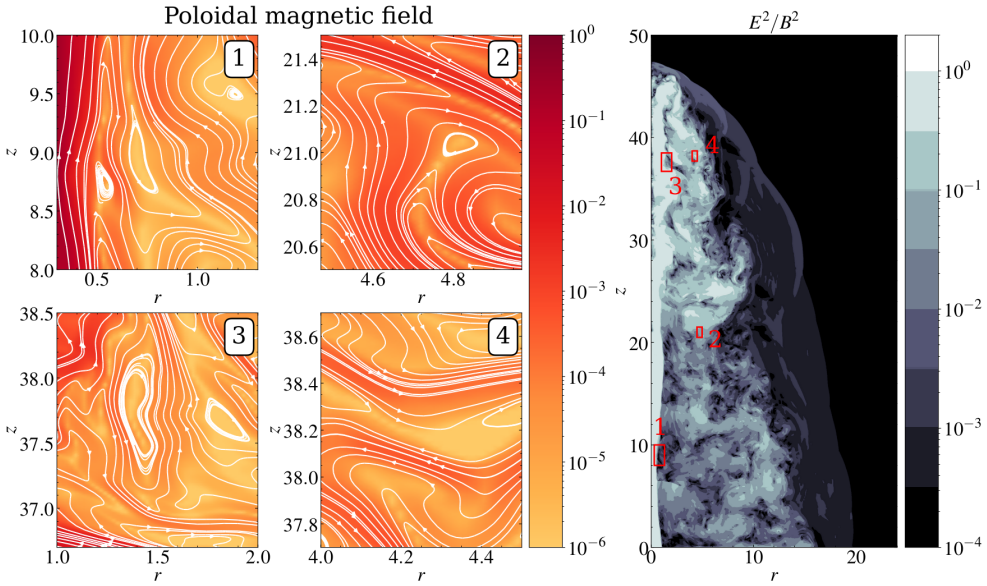

Figure 1: Current sheet forming in the turbulent jet region for the case $\eta = 10^{-3}$ at $t = 300$.

The value of the pressure p_j is retrieved by imposing the Mach number $M = 6$. The thermal pressure distribution inside the jet can then be recovered assuming radial momentum equilibrium. Unless stated otherwise, the electric field is initialized inside the jet to its ideal value $\vec{E} = -\vec{v} \times \vec{B}$. More details can be found in Mattia et al. [5], Mignone et al. [10].

3. Results

In this section, we report some results of our simulations which have also been presented in Mattia et al. [5].

3.1 Formation of resistive current sheets

Here we investigate the formation of current sheets in the simplest resistivity model (i.e. $\eta = 10^-3$ is constant in time and space). In Figure 1 (right panel) we have reported the ratio between the electric and magnetic energy, which indicates where magnetic reconnection would be able to accelerate non-thermal particles more efficiently. As expected, the most promising acceleration sites are relocated close to the jet spine and in the turbulent regions where the jet and the ambient medium have strongly interacted. We have then isolated four different regions (left panels) where the magnetic field shows an inversion of its polarity and becomes prone to the formation of relativistic current sheets (which are a primary ingredient for magnetic reconnection). Each region shows one or multiple inversions of the magnetic field lines due to the turbulence within the jet, and the consequent tearing instability leading to the plasmoids. Despite the lack of resolution required to properly resolve the complex internal structure of the magnetic islands, we can select several portions of each region where the magnetic field polarity is suitable for magnetic reconnection and plasmoid instability, allowing us to properly detect the X- and O-points in current sheets (as shown in the zoomed panels). All the panels selected (but the top right, number 2) show

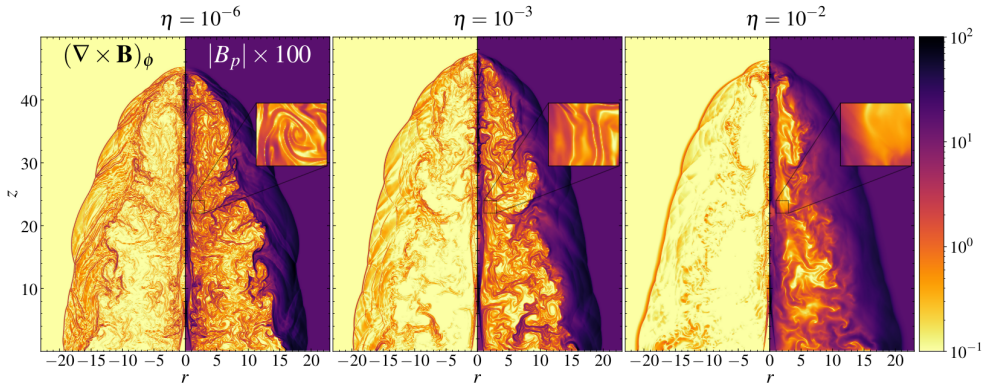

Figure 2: Toroidal component of the magnetic field's curl (left panel blocks, representing a proxy for the toroidal current) and poloidal magnetic field (right panel blocks) for different values of the resistivity.

an average magnetization between 0.1 and 10, since a lower magnetization may not lead to the formation of plasmoids [2].

3.2 The impact of a constant resistivity

In order to more systematically detect possible reconnection sites, we focus on the structure of the poloidal magnetic field and its curl, that is the non-relativistic current $\vec{J}_\phi = (\nabla \times \vec{B})_\phi$, (see Figure 2) as often done in the literature, even by devising specific detectors based on this quantity [11]. As a first consideration, we point out that current sheets and magnetic islands can also appear in simulations without an explicit physical resistivity (ideal MHD), due to the intrinsic and unavoidable diffusivity of the numerical schemes. Because of the lack of turbulence caused by the physical resistivity in the most dissipative case with $\eta = 10^{-2}$, the formation of current sheets is largely reduced compared with the other two cases. In particular, thicker current sheets are formed only in selected regions, e.g. near the axis, the jet head, and between the jet material and the bow shock. Conversely, a lower resistivity leads to more ubiquitous and thinner current sheet regions. The strong dependence of the formation of current sheets with the higher magnetization maintained only in the lower resistivity runs, is promising, given that astrophysical plasmas are expected to be quasi-ideal and favorable for the turbulent reconnection scenario.

3.3 Variable resistivity models

A constant resistivity profile, albeit a very simple and effective strategy, may not consistently model the differences between the jet and the ambient medium. The assumption of a resistivity confined in the jet is justified [12] by the turbulent (and thus resistive) nature of the accretion disks. For instance, Qian et al. [13], Vourellis et al. [14] assumed a resistivity caused by the thin accretion disk rotation which triggers the magnetorotational instability. A similar assumption is made by Bugli et al. [15], Tomei et al. [16] in the context of mean-field dynamo in thick accretion tori. It is therefore natural to expect that the turbulent/resistive nature of the accretion flow is present also in the outflow at a greater distance from the accreted matter. A simple yet effective way to model a more consistent diffusivity profile is to relate it to the passive scalar tracer f (Tr-case):

$$\eta = \max\left(10^{-6}, 10^{-3} f\right). \tag{1}$$

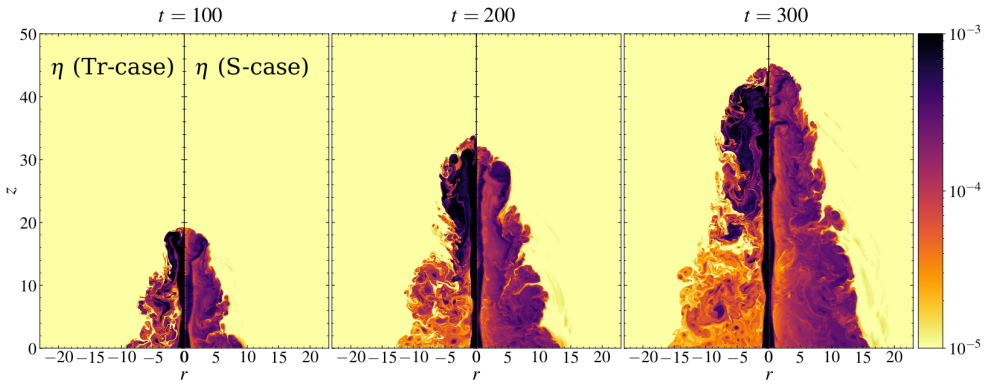

Figure 3: Resistivity computed at different times ($t = 100, 200, 300$respectively in the left, middle, and right panel blocks) with the two different variable resistivity models (respectively, Tr-case on the left panels and S-case on the right panels).

Another more consistent resistivity profile is computed, similar to Fendt & Čemeljić [12], by fixing the Lundquist number S (S-case):

$$\eta = \frac{v_A r_j}{S} \tag{2}$$

where v_a is the local Alfvén speed and r_j is adopted as a typical length scale of our system. Here we set $S = 10^3$ to properly mimic a physical resistivity comparable with the previous cases. By computing the average value of the jet resistivity (as shown in Fig. 3), we notice a different saturation of such value. More specifically, already at $t \sim 30$, the average jet resistivity has reached a value of 2.5×10^{-4} for the S-case, which remains quite constant through the rest of the simulation. On the other hand, the average jet resistivity in the Tr-case starts with a value of $\sim 10^-3$ as the jet is injected ($t \geq 0$) since the jet and ambient matter have not started to interact yet; around $t \sim 100$, the jet and the ambient medium have already interacted and the average jet resistivity slowly converges to 4.5×10^{-4} until the end of the simulation.

4. Conclusions

In this work, we presented a numerical study, in the regime of resistive relativistic magnetohydrodynamics (RRMHD), of astrophysical relativistic jets endowed with both poloidal and toroidal magnetic field components propagating through a uniform magnetized medium. We combined a high-resolution grid in cylindrical coordinates with high-order numerical algorithms and realistic physical assumptions to achieve the best level of refinement while preserving the robustness required to overcome the numerical issues often arising when simulating relativistic flows in a strongly magnetized regime. The following summarizes our approaches and results:

- the combination of high-order numerical algorithms and high resolution enables us to find with increased accuracy the formation of X- and O-points within the jets, despite the lack of resolution required to resolve the particles' acceleration scales. However, selected zones of the large-scale jets can provide more consistent recipes to investigate the reconnection process at smaller scales;

- we have investigated the role of a constant (in space and time) resistivity coefficient. More specifically, we found that a high resistivity coefficient suppresses almost completely the turbulence in the propagating jet and therefore the formation of relativistic current sheets. Conversely, a lower resistivity triggers the formation of multiple zones that could be prone (in terms of magnetization and field topology) to plasmoid instability;
- we have also adopted and compared more consistent diffusivity models with a variable coefficient η, one based on a passively evolved scalar jet tracer, and another one fixing a constant value for the Lundquist number. Such models feature a more refined level of turbulence with respect to the case of intermediate constant diffusivity, consistent with the fact that the resistivity in the jet varies in the range $10^{-5} \leq \eta \leq 10^{-3}$.

Despite the collisionless resistivity typical of astrophysical plasmas being orders of magnitude higher than any physical or numerical resistivity here presented, this study represents an attempt to control more accurately the unavoidable numerical diffusion present in every MHD simulation. By adopting this approach, we aim to assess more quantitatively the impact of dissipative processes in more specific astrophysical sources, e.g. the short GRB jet GRB 170817A (where the intricate interplay between the magnetized environment and the jet makes it a perfect ambient for dissipative processes to take place, as shown in Pavan et al. 17), in the near future.

References

[1] Del Zanna, L., Papini, E., Landi, S., et al. 2016, MNRAS, 460, 3753.

[2] Ripperda, B., Porth, O., Sironi, L., et al. 2019, MNRAS, 485, 299.

[3] Loureiro, N. F. & Uzdensky, D. A. 2016, Plasma Physics and Controlled Fusion, 58, 014021.

[4] Medina-Torrejón, T. E., de Gouveia Dal Pino, E. M., & Kowal, G. 2023, ApJ, 952, 168.

[5] Mattia, G., Del Zanna, L., Bugli, M., et al. 2023, A&A, 679, A49.

[6] Mignone, A., Bodo, G., Massaglia, S., et al. 2007, ApJS, 170, 228.

[7] Mignone, A., Mattia, G., Bodo, G., et al. 2019, MNRAS, 486, 4252.

[8] Mizuno, Y. 2013, ApJS, 205, 7.

[9] Palenzuela, C., Lehner, L., Reula, O., et al. 2009, MNRAS, 394, 1727.

[10] Mignone, A., Ugliano, M., & Bodo, G. 2009, MNRAS, 393, 1141.

[11] Nurisso, M., Celotti, A., Mignone, A., et al. 2023, MNRAS, 522, 5517.

[12] Fendt, C. & Čemeljić, M. 2002, A&A, 395, 1045.

[13] Qian, Q., Fendt, C., & Vourellis, C. 2018, ApJ, 859, 28.

[14] Vourellis, C., Fendt, C., Qian, Q., et al. 2019, ApJ, 882, 2.

[15] Bugli, M., Del Zanna, L., & Bucciantini, N. 2014, MNRAS, 440, L41.

[16] Tomei, N., Del Zanna, L., Bugli, M., et al. 2020, MNRAS, 491, 2346.

[17] Pavan, A., Ciolfi, R., Kalinani, J. V., et al. 2023, MNRAS, 524, 260.